Theta but not beta power is positively associated with better explicit motor task learning

van der Cruijsen, Joris; Manoochehri, Mana; Jonker, Zeb D.; Andrinopoulou, Eleni Rosalina; Frens, Maarten A.; Ribbers, Gerard M.; Schouten, Alfred C.; Selles, Ruud W.

DOI
10.1016/j.neuroimage.2021.118373

Publication date
2021

Document Version
Final published version

Published in
NeuroImage

Citation (APA)
van der Cruijsen, J., Manoochehri, M., Jonker, Z. D., Andrinopoulou, E. R., Frens, M. A., Ribbers, G. M., Schouten, A. C., & Selles, R. W. (2021). Theta but not beta power is positively associated with better explicit motor task learning. *NeuroImage*, *240*, Article 118373. https://doi.org/10.1016/j.neuroimage.2021.118373

NeuroImage 240 (2021) 118373

Contents lists available at ScienceDirect

NeuroImage

journal homepage: www.elsevier.com/locate/neuroimage

Theta but not beta power is positively associated with better explicit motor task learning

Joris van der Cruijsen[a,*], Mana Manoochehri[b], Zeb D. Jonker[a,c,d],
Eleni-Rosalina Andrinopoulou[e], Maarten A. Frens[c], Gerard M. Ribbers[a,d], Alfred C. Schouten[b,f],
Ruud W. Selles[a,g]

[a] *Erasmus MC, University Medical Center Rotterdam, Department of Rehabilitation Medicine, 3015 GD Rotterdam, Netherlands*
[b] *Delft University of Technology, Department of Biomechanical Engineering, 2628 DS Delft, Netherlands*
[c] *Erasmus MC, University Medical Center Rotterdam, Department of Neuroscience, 3015 GD Rotterdam, Netherlands*
[d] *Rijndam Rehabilitation Center, 3015 LJ Rotterdam, Netherlands*
[e] *Erasmus MC, University Medical Center Rotterdam, Department of Biostatistics, 3015 GD Rotterdam, Netherlands*
[f] *University of Twente, Department of Biomechanical Engineering, 7522 NB Enschede, Netherlands*
[g] *Erasmus MC, University Medical Center Rotterdam, Department of Plastic and Reconstructive Surgery and Hand Surgery, 3015 GD Rotterdam, Netherlands*

ARTICLE INFO

Keywords:
EEG
Motor learning
Independent component analysis

ABSTRACT

Neurophysiologic correlates of motor learning that can be monitored during neurorehabilitation interventions can facilitate the development of more effective learning methods. Previous studies have focused on the role of the beta band (14–30 Hz) because of its clear response during motor activity. However, it is difficult to discriminate between beta activity related to learning a movement and performing the movement. In this study, we analysed differences in the electroencephalography (EEG) power spectra of complex and simple explicit sequential motor tasks in healthy young subjects. The complex motor task (CMT) allowed EEG measurement related to motor learning. In contrast, the simple motor task (SMT) made it possible to control for EEG activity associated with performing the movement without significant motor learning. Source reconstruction of the EEG revealed task-related activity from 5 clusters covering both primary motor cortices (M1) and 3 clusters localised to different parts of the cingulate cortex (CC). We found no association between M1 beta power and learning, but the CMT produced stronger bilateral beta suppression compared to the SMT. However, there was a positive association between contralateral M1 theta (5–8 Hz) and alpha (8–12 Hz) power and motor learning, and theta and alpha power in the posterior mid-CC and posterior CC were positively associated with greater motor learning. These findings suggest that the theta and alpha bands are more related to motor learning than the beta band, which might merely relate to the level of perceived difficulty during learning.

1. Introduction

Motor learning—defined as acquiring new skills, improving existing skills, or regaining/reinforcing skills through practice—is critical for developing motor function at all stages of life Magill and Anderson (2017). However, the neurophysiology of motor learning is complex and not fully understood. Differences in brain structure and function (Tomassini et al., 2011) and genetic factors (McHughen et al., 2010) contribute to the variability in motor learning capacity amongst healthy individuals. To better understand this variability, investigators have analysed neurophysiologic correlates of motor learning by electroencephalography (EEG)/magnetoencephalography (MEG). This has allowed real-time monitoring of motor learning during rehabilitation (Amo et al., 2017; Mane et al., 2019), the development of brain-computer interfaces Saha and Baumert (2020), and the improvement of non-invasive brain stimulation techniques (Thut et al., 2017).

Complex sequential learning tasks involve working memory, attention, and cognitive control and are easy to combine with neuroimaging. Previous imaging studies have revealed the involvement of various brain regions in complex motor learning, including the dorsolateral prefrontal cortex (Ghilardi et al., 2000), anterior cingulate cortex (ACC) (Ghilardi et al., 2000; Jueptner et al., 1997), basal ganglia Brittain and Brown (2014), supplementary motor area, and primary motor cortex (M1) (Ashe et al., 2006). M1 beta-band activity (14–30 Hz) is known to modulate with motor execution (Pfurtscheller et al., 1996) and has been related to motor learning in studies with healthy subjects (Espenhahn et al., 2019; Meziane et al., 2015; Pollok et al., 2014) and

---

[*] Corresponding author.
E-mail address: j.vandercruijsen@erasmusmc.nl (J. van der Cruijsen).

https://doi.org/10.1016/j.neuroimage.2021.118373.
Received 22 November 2020; Received in revised form 2 July 2021; Accepted 6 July 2021

patients suffering from neurological disorders (Espenhahn et al., 2020; Meissner et al., 2018). Studies with Parkinson's disease patients indicate reduced motor learning capacity results from affected basal ganglia-thalamo-cortical network, reflected by enhanced beta power compared to healthy individuals (Meissner et al., 2018; Weiss et al., 2015). In addition to the beta band, motor learning has also been suggested to be related to theta (5–8 Hz), alpha (8–12 Hz), and gamma (60–90 Hz) frequency band modulation (Boonstra et al., 2007; Meissner et al., 2018; Sugata et al., 2018; Zhuang et al., 1997). However, none of these studies controlled for brain activity associated with performing the movement; therefore, it is unclear whether the activity is specifically associated with motor learning.

To address this point, this study aimed to investigate EEG-based neurophysiologic correlates of motor learning that solely reflect learning the movement by controlling for performing the movement. To this end, we used a complex motor learning task (Reis et al., 2009) that induces motor learning (Coxon et al., 2014) and a simplified motor task that requires very similar movement but induces little or no learning. During both tasks, participants applied a pinch force to a force transducer to move a cursor according to a fixed complex or simple sequence displayed on a computer screen. We administered both motor learning tasks in a within-subjects design to identify neurophysiologic correlates specific to online motor learning and not to motor movement. We do so by calculating the difference in learning between the complex motor learning task and the simple motor learning task and comparing these with differences in EEG power in the theta, alpha, and beta frequency bands. Although motor control also involves the gamma band (Nowak et al., 2018), this is typically through phase-amplitude coupling (PAC) with slower oscillations (Canolty et al., 2006; Chacko et al., 2018; Osipova et al., 2008), which is beyond the current analysis scope.

2. Methods

2.1. Participants

Twenty healthy volunteers participated in this experiment (age: 18–30 years, 13 females). Due to the explorative nature of the study, no a priori sample size estimation was performed. All participants provided written, informed consent before the experiment. Participants were self-reported as right-handed and free of any neuromuscular disorders. The study was approved by the medical ethics review board of the Erasmus University Medical center (NL64529.078.18) and conducted in accordance with the Declaration of Helsinki (2013).

2.2. Experimental design

Participants performed 2 sequential visual isometric pinch tasks in a counterbalanced order: a complex motor task (CMT) that has been shown to induce learning over many repetitions and a simple motor task (SMT) which required little to no learning over repetitions. The CMT was adapted from previous research demonstrating that participants showed an approximately linear improvement within and over multiple sessions without reaching a plateau (Coxon et al., 2014; Reis et al., 2009). The SMT was based on the CMT, but the task was made easier so that participants would reach an early learning plateau.

In both tasks (Fig. 1 panel A and B), participants had to move a cursor from the "home" position to a target on the screen by pinching a force transducer between the right thumb and index finger. Between targets, the participant had to move the cursor back to the home position by releasing the force on the transducer. In the CMT, a trial consisted of moving the cursor to 1 of 5 targets sequentially, whereas in the SMT, the participant had to reach the same target 5 times. The relationship between pinch force and cursor position varied according to the maximum pinch force that was applied. In the CMT, the relationship was logarithmic: for low displacement, a small force increase produced a large displacement, and the displacement decreased with increasing pinch force. Because of the nonlinear nature of the force–cursor position relationship, motor learning was required to perform the task well (see Fig. 1 panel D). In contrast, in the SMT the relationship between force and cursor position was linear and there was only a single, wide target; as such, it required little to no learning to perform the task well. We controlled for performing the movement in the CMT by ensuring that the average force required to reach five targets in a single trial was similar for both tasks.

A metronome (80 beats/min) provided cues for the start of the trial and the pace at which participants had to reach the target(s). The metronome was used to constrain the single-trial duration and to align trials to facilitate the EEG analysis. A countdown of 3 high-pitched beeps indicated the start of the trial. A synchronisation trigger was sent to the EEG amplifier upon the third high-pitched beep to indicate the start of each trial, set as $t = 0$. After trial onset, as indicated by the metronome, participants had 750 ms to reach each target. A target was successfully reached if the maximum cursor position within a 50 ms time window around the metronome beep was within a 50-pixel window around the target's centre (see Fig. 1 panel C). This dichotomous measure was used as a single measure suitable to quantify performance in both the CMT and SMT. Numeric measures such as accuracy, precision, or error rate were not considered suitable, as they require a fixed reference point that cannot be defined for the SMT. Participants were instructed to reach correctly as many targets as possible in both tasks.

The CMT and SMT started with three practice blocks to familiarise the participant with the task, followed by 20 blocks of 10 trials. Consecutive blocks were separated by 30 s breaks and consecutive trials by 2 s. After each block, the percentage of successfully reached targets was presented to the participant. Furthermore, the percentage successfully reached targets per target for the latest block was provided.

For both tasks, learning was defined as the slope of the best fitting linear line through all the individual performance points per block. Previous studies employing the CMT describe subjects improve approximately linearly over time (Coxon et al., 2014; Reis et al., 2009), making the slope a suitable quantity to describe learning. As such, positive slopes indicated learning, whereas negative slopes indicated a reduction in performance over time. The difference in slopes between the CMT and SMT was the final measure used for motor learning in the subsequent analysis to correct for (unexpected) learning in the SMT.

2.3. EEG recordings

EEG was performed throughout the experiment using 62 Ag–AgCl electrodes aligned according to the international 10–5 system (Oostenveld and Praamstra, 2001) in an EEG gel head cap (TMSi, Enschede, The Netherlands). Two additional electrodes were placed at the right temple and slightly above the nasion to record horizontal and vertical eye movements, respectively. The ground electrode was positioned at the right mastoid. A bipolar montage was used to record muscle activity of the right first dorsal interosseous muscle. The impedance of all electrodes was maintained below 5 kOhm. All electrophysiologic data were collected at 2048 Hz, referenced to the common average, using a biosignal amplifier (Refa 128; TMSi) that received a synchronisation signal at the start of each CMT or SMT trial.

2.4. EEG analysis

2.4.1. EEG preprocessing

All data were processed using EEGLAB v14 (Delorme and Makeig, 2004) in MATLAB (Mathworks, Natick, MA, USA). Each task's data were downsampled to 1024 Hz and then bandpass-filtered between 1 and 60 Hz (order: 3380) using EEGLAB's built-in finite impulse response filter. A notch filter was applied at 50 Hz (48–52 Hz, order: 1690) to remove apparent line noise identified in the power spectra of the data. The data of both tasks were concatenated to apply all the following steps on both the CMT and SMT data. Most importantly, this ensured that

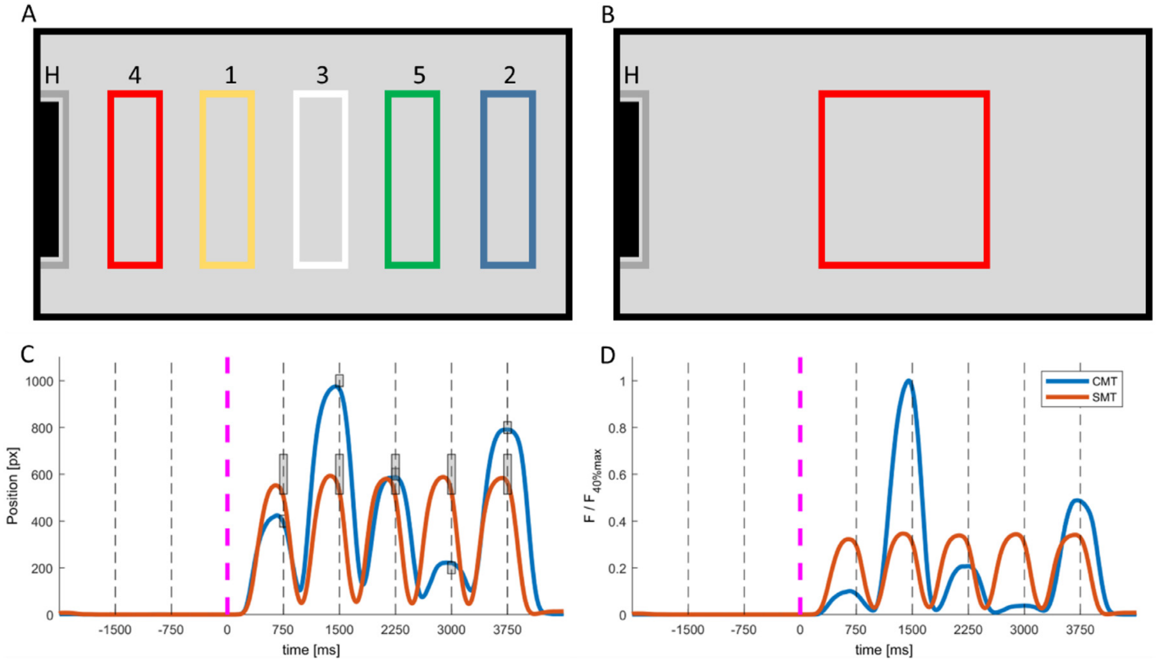

Fig. 1. Overview of the experimental tasks. Panel A shows the complex motor task, in which participants had to move the black cursor from the 'home' position, indicated with 'H', in sequence to targets 1 to 5. Panel B: the simple motor learning task, in which participants had to move the black cursor inside the red target five consecutive times. Panel C and D show the average cursor position over time (C) and average force over time (D), respectively, of a single subject during the complex (blue) and simple (red) motor learning task. Dashed lines indicate a beep of the metronome. The magenta dashed line indicates the metronome beep corresponding to the start of the trial, at which the EEG amplifier received a synchronisation trigger. Black dashed lines succeeding the synchronisation trigger indicate metronome beeps at which targets had to be reached. The grey shaded areas indicate the margins in time (x-axis) and position (y-axis) for which the cursor position successfully reached the target.

the source localisations were equal for both tasks to allow between-task comparisons of the EEG. Bad channels were detected by visual inspection and rejected, and the remaining channels were re-referenced to the common average. On average, 1.4 ± 1.54 (mean±standard deviation) electrodes were rejected.

2.4.2. *Source-level analysis*

For source-level analysis, the following steps were carried out on a copy of the continuous preprocessed data. The data were downsampled to 256 Hz to reduce the computation time of subsequent steps, and data points outside the window of −2 to 5 s around the synchronisation trigger ($t = 0$) were removed. To keep as much data as possible during artefact rejection, we first split the remaining data into 0.5 s epochs. Then, a built-in automated rejection protocol was applied to remove bad epochs with data points above the epoch mean±6 times the standard deviation of the full 0.5 s epoch.

Adaptive mixture independent component analysis (ICA) (Palmer et al., 2008) was performed on the clean 0.5 s data epochs of individual subjects to reconstruct the source-level activity of the recorded data. Due to our experimental design, EEG signals comprise a mixture of task-related sources of motor, visual, and auditory activity but also unrelated activity from artefacts such as eye movement and muscle activity. ICA is a reliable tool for separating different sources of cortical activity from each other and artifacts (Delorme et al., 2012). ICA information (weight and sphering matrix) was copied back to the continuous preprocessed dataset. From this dataset, epochs of −2 to 5 s around the synchronisation trigger ($t = 0$) were generated to obtain full-trial component activations. The full trials were cleaned by applying an automated rejection algorithm to the component activations to remove trials containing data points larger than the trial mean±6 standard deviations. Then, we verified by visual inspection that no noisy trials were included in the following steps. On average, 189.8 ± 5.5 and 190.3 ± 6.2 trials were included in the analysis for the CMT and SMT, respectively (mean±sd). Horizontal electrooculogram (EOG) components were visually identified on the time course of the signal that was most highly correlated with cursor position during the task. Vertical EOG components showed blinking only up to −1.5 s before the start of the trial and at the end of each trial. Both horizontal and vertical EOG components were discarded from the analysis.

Source localisation was performed on the independent components by fitting equivalent dipoles (DIPFIT 2.3 plugin for EEGLAB) to the cleaned component activations, simulated on a 3-compartment boundary element model derived from the MNI canonical template brain. The model consisted of compartments for scalp, skull, and brain with corresponding conductivities of 0.33 S/m, 0.0041 S/m and 0.33 S/m, respectively. A template brain with fixed conductivities results in approximate locations of the dipolar sources that generate the reconstructed source-level activity. Only components that could be fitted as a dipole in the brain with a residual variance <10% (Delorme et al., 2012) and with $1/f$ power spectra were considered for further analysis. All remaining components of all subjects were clustered by k-means clustering of the dipole location Arthur and Vassilvitskii (2007) by minimising the distance between individual dipole locations and k means. The number of generated clusters was equal to the number of included components divided by the number of subjects. We set a minimum of 10 participants per cluster to be retained for further analysis. The coordinates of the cluster means were used to approximate the brain region represented by the cluster based on the nearest grey matter point in Talairach coordinates (Lancaster et al., 2000, 1997).

Time–frequency representations of full trials of independent components included in the selected clusters were calculated based on Morlet wavelet convolutions at 100 logarithmically distributed frequency steps between 3 and 60 Hz and a linearly increasing number of cycles from 3 to 16. Time-frequency decompositions were calculated per subject per for both the CMT and SMT trials. Single trials were normalised by dividing by the mean full single-trial power spectrum before averaging over trials to reduce sensitivity to noise Grandchamp and Delorme (2011). Multiple components of the same subject within a cluster were first averaged before averaging over all subjects.

Average power per motor task was calculated during trial execution (t = [0, 3750] ms) within theta (5–8 Hz), alpha (8–12 Hz), and beta (14–30 Hz) frequency bands. We defined EEG power enhancement as event-related synchronization (ERS) and power suppression as event-related desynchronization (ERD). The EEG power ratio between CMT and SMT for every cluster was calculated and subtracted by 1 for the subsequent statistical analysis to correct for any unexpected learning in the SMT. As such, a power ratio of 0 indicates that EEG power was equal during both tasks. Positive values indicate that EEG power for a specific frequency band/cluster combination was higher during CMT compared to SMT.

2.5. Statistical analysis

We analysed the learning rate differences in the behavioural data using a linear mixed-effect model with main effects for *task* and *block* and an interaction term $task \times block$. Furthermore, the linear mixed-effects model included nested random intercepts and random (linear) slopes per subject per condition to describe between-subject variability in starting performance and learning rate. Using this model, we investigated the differences between the CMT and SMT in mean starting performance (main effect *task*) and learning rate (main effect *block* and interaction term $task \times block$).

To identify whether EEG correlates on motor learning, we fitted a generalised estimating equation (GEE) model. In the GEE model, EEG band power was the dependant variable. The GEE approach was used since the regression parameters are sensitive to random-effect assumptions. Given our objective is to investigate the population average of EEG power with covariate groups, we assume a GEE with robust sandwich estimators (Hubbard et al., 2010). We included main effects for the independent variables *cluster, frequency band,* and *learning* in the model. Due to the sample size, we limited interactions to only the two-way interaction terms $cluster \times learning$ and $cluster \times frequency$. We computed the GEE's marginal effects to explore the relationship between learning and EEG band power per cluster. The marginal effects estimate both an intercept and a slope to predict how EEG band power per cluster relates to motor learning. Given the nature of our measure for learning (the difference in learning slopes between CMT and SMT) and EEG power (the ratio $CMT/SMT\ - 1$), significant positive slopes indicate that EEG power from a particular frequency band/cluster is positively associated with motor learning. Furthermore, significant intercepts indicate that the mean power in a frequency band – cluster combination was different between the CMT and SMT. All statistical analysis were performed in R 4.0.3 (R Core Team, 2019) and the packages *geepack* (Halekoh et al., 2006) and *nlme* (Pinheiro et al., 2020).

2.6. Data and code availability statement

The data that support the findings of this study are available from the corresponding author, JC, upon reasonable request.

3. Results

3.1. Motor learning

The main effects of the linear mixed effects model revealed that mean starting performance in the SMT (β_0 = 78.5%, SE = 2.414, $p < 0.001$) was significantly higher than during the CMT (β_0 = −53.4%, SE = 3.41,$p < 0.001$). Furthermore, mean performance significantly increased over blocks in the SMT (main effect for *block*: β_1 = 0.406, SE = 0.128, p = 0.002), but more during the CMT (interaction term $block \times task$: β_1 = 0.529, SE = 0.181, p = 0.003). The random effects (Fig. 2) showed that 16/20 subjects (80%) had a steeper slope during the CMT compared to the SMT, indicating a greater degree of learning in the former task.

3.2. EEG

3.2.1. Source-level activity

EEG channel activations were localised and clustered into 5 distinct areas (Table 1 and Fig. 3). The cluster centres were approximated to the contralateral (c)M1 and ipsilateral (i)M1 and CC (anterior mid-CC [aMCC], posterior [p]MCC (Vogt, 2016), and posterior CC [PCC]).

Visual inspection of the mean time-frequency decompositions of the bilateral M1 clusters shows during both tasks alpha and beta ERS during task preparation (t = [-2, 0]) and beta and alpha ERD during task execution t = ([0, 3.75]). For the aMCC cluster, theta ERD was observed during preparation, followed by theta ERS after trial onset. Theta ERS was time-locked to the auditory cue at 750 ms intervals after trial onset during the execution phase. In the SMT, these theta bursts were absent. In the pMCC cluster, theta ERS bursts were time-locked with the metronome to 750 ms intervals after trial onset in the mean time-frequency decompositions for both tasks. The PCC cluster exhibited an alpha ERD and theta ERS burst-like pattern time-locked to the metronome, and trial execution was also accompanied by beta ERD in both motor learning tasks. Interestingly, the alpha ERD bursts preceded the metronome beeps, whereas theta ERS bursts succeeded the metronome, suggesting that the activity was related to distinct parts of the motor task.

3.2.2. EEG–task performance

Analysis of the GEE model showed no main effect of learning (β_1 = −0.008, SE = 0.009, p = 0.392), but significant interaction effects between learning and the theta (β_1 = 0.023, SE = 0.007, $p < 0.001$) and alpha frequency band (β_1 = 0.025, SE = 0.007, $p < 0.001$). Additionally, there was a significant interaction between the PCC cluster and learning (β_1 = 0.036, SE = 0.017, p = 0.036).

In addition to the main effects and interaction terms, we computed the GEE's model marginal effects to explore the relationship between learning and frequency band per cluster (see Fig. 4). The marginal effects indicated that in the cM1, learning was positively associated with both theta (β_1 = 0.047, CI = [0.010, 0.085]) and alpha power (β_1 = 0.049, CI = [0.002, 0.097]) but not with beta power (β_1 = 0.024, CI = [-0.020, 0.068]). Power in iM1 was not associated with higher learning rates for any of the analysed frequency bands. However, mean differences in EEG power were found in cM1 for the beta (β_0 = -0.061, CI = [-0.102,-0.020]) band. In iM1, a mean difference was found for both the alpha (β_0 = −0.038, CI = [−0.068, −0.008]) and beta (β_0 = −0.056, CI = [−0.085, −0.026]), indicating a difference between the motor learning tasks not translating into higher learning rates.

For the cingulate cortex clusters, aMCC power was not associated with better learning. However, theta (β_1 = 0.027, CI = [0.011, 0.043]) and alpha (β_1 = 0.029, CI = [0.010, 0.048]) power in the pMCC and theta (β_1 = 0.051, CI = [0.021, 0.082]) and alpha (β_1 = 0.054, CI = [0.017, 0.090]) power in the PCC were both positively associated with motor learning. Full details of the analysis of the marginal effects can be found in Supplementary Table 1.

4. Discussion

Our study design was verified by participants learning more in the CMT than the SMT, although most participants also improved significantly in the SMT. In our evaluations of between-subject differences in learning and differences in EEG power, a higher degree of motor learning was positively associated with higher theta and alpha power in cM1, the pMCC and PCC. Bilateral M1 beta power was higher during the CMT than the SMT, but not associated with higher motor learning.

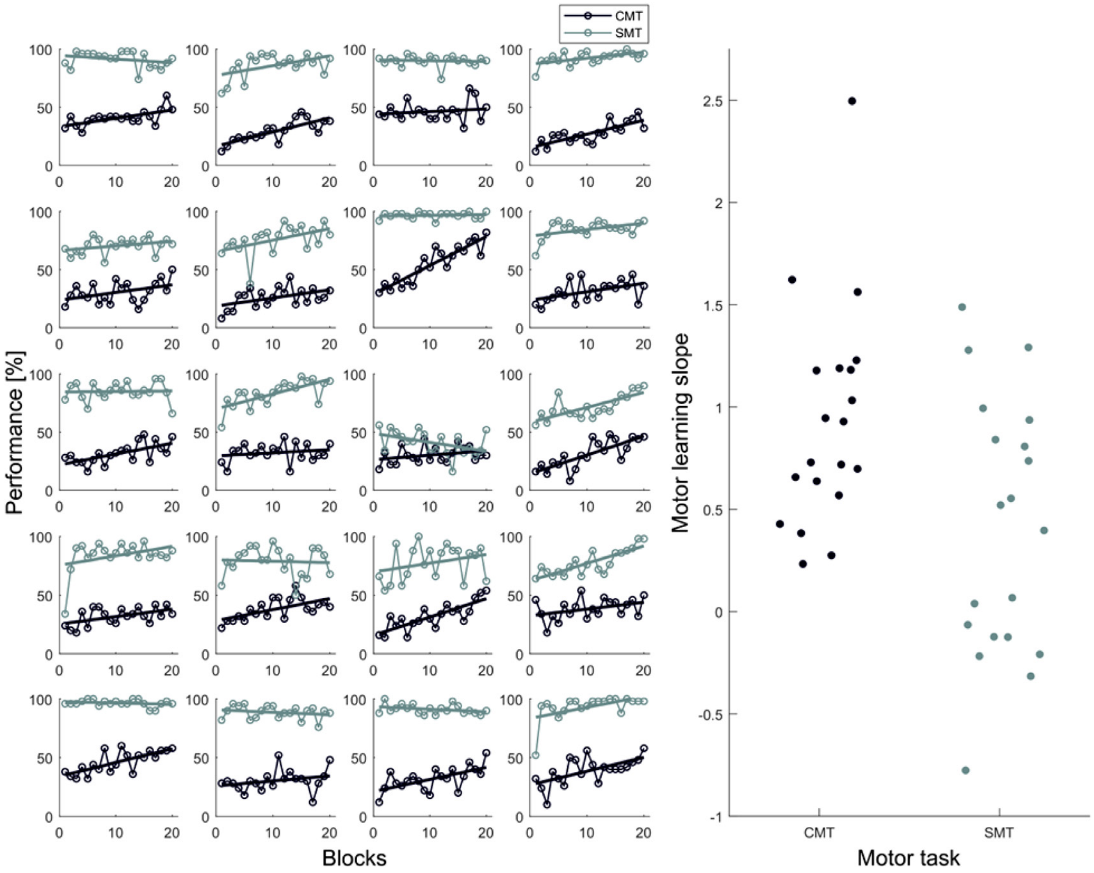

Fig. 2. Left panel: performance (y-axis) per block (x-axis) of individual subjects. Performance in the CMT and SMT is shown in black and grey, respectively. The random intercept and slope for each condition indicate the starting performance and the degree of motor learning. Right panel: motor learning slopes (y-axis) sorted by task (x-axis).

Table 1
Source localisation results.

Cluster	Number of subjects (components)	Coordinates of mean dipole location cluster centres, mm X	Y	Z	Nearest Brodmann area
cM1	14 (19)	−43	−12	41	BA4
iM1	15 (21)	40	−9	39	BA6
aMCC	15 (18)	−3	28	23	BA32
pMCC	14 (17)	3	6	46	BA32
PCC	17 (23)	8	−32	39	BA31

Abbreviations: aMCC, anterior mid-cingulate cortex; cM1, contralateral primary motor cortex; iM1, ipsilateral primary motor cortex; pMCC, posterior mid-cingulate cortex; PCC: posterior cingulate cortex.

4.1. M1

Controlling for EEG activity related to performing a movement, we found a positive relationship between motor learning and M1 theta and alpha power, but not beta power. The positive association between motor learning and cM1 theta power observed in our study has been previously reported (Meissner et al., 2018). Moreover, increasing theta power through neurofeedback was shown to improve learning in an explicit motor sequence task (Rozengurt et al., 2016). Both studies suggested that the relationship between motor learning and theta power was related to memory consolidation. However, in the present study, theta power relates to increased ongoing motor learning in a complex motor learning task. The nature of the CMT we applied requires changes in the motor plan, involving multiple brain regions from the motor network (Doyon et al., 2009). Therefore, the relationship between motor learning and theta band activity fits with a previous report that relates the theta band to motor plan updates and communication between multiple brain regions (Caplan et al., 2003; Pellegrino et al., 2018). More specifically, theta band's role in communication between distant cortical regions has been shown by phase-amplitude coupling (PAC) with the gamma frequency band (Canolty et al., 2006), with higher theta power resulting in higher PAC. Additionally, M1-targeted gamma transcranial alternating current stimulation phase-locked to the theta band resulted in enhanced motor learning in an explicit motor learning task in healthy subjects (Akkad et al., 2019). In PD patients, M1 tACS enhanced cortical plasticity, reducing the effects of the impaired basal ganglia-thalamo-cortical network (Guerra et al., 2020). Given these reports, we believe that the positive association between learning and theta power in our study could reflect increased cortical plasticity by higher coupling with the gamma band and thus promoting motor learning.

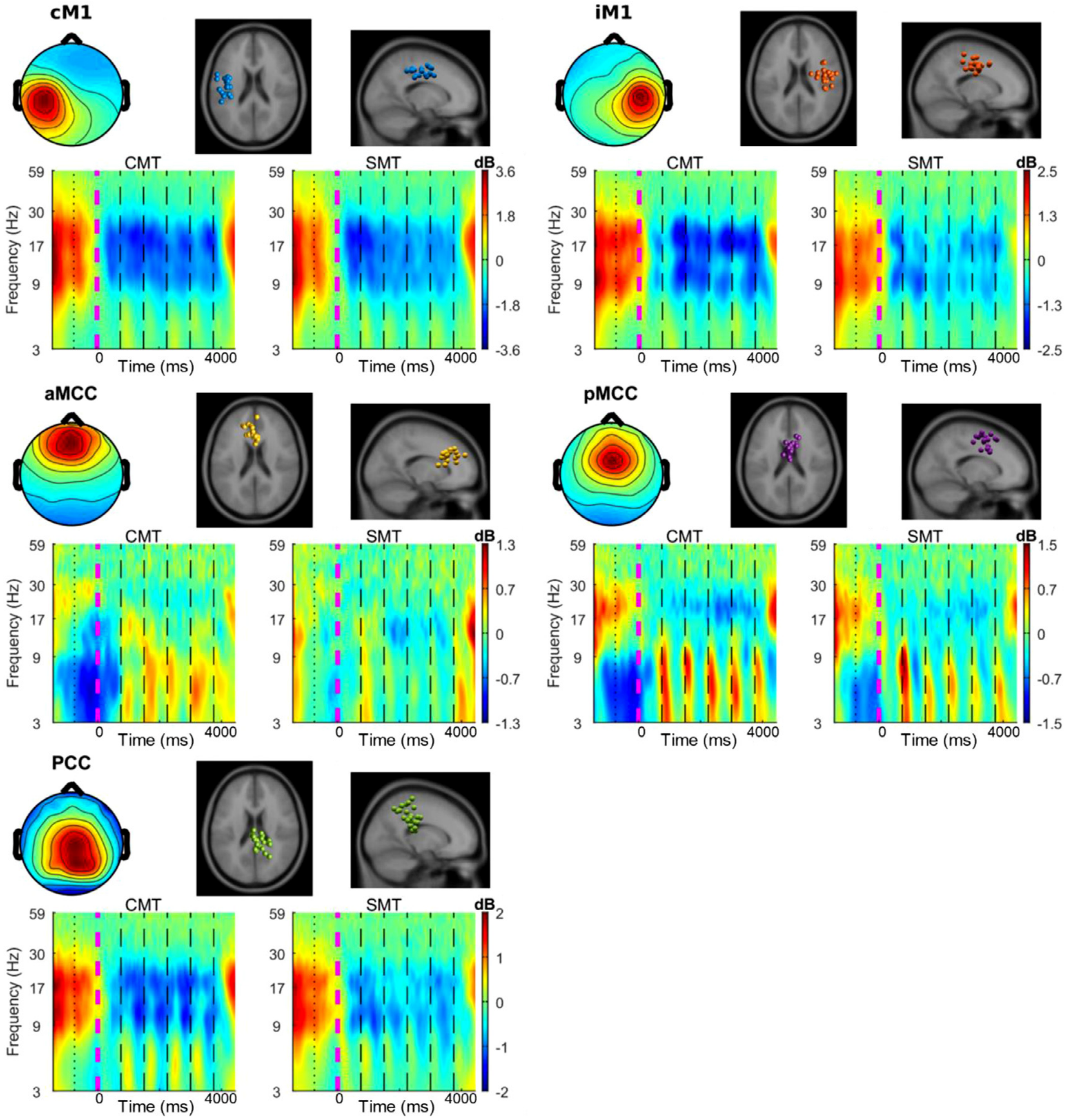

Fig. 3. Cluster-wise visualisation of the time–frequency representation. For each cluster reported in Table 2, the upper row shows the scalp maps and positions of individual dipoles fitted in the standardised MNI152 brain. The lower row shows the time–frequency representations for CMT, SMT. The dashed magenta line indicates the start of the trial. Succeeding dashed black lines correspond to metronome beeps at which participants had to reach the targets in the task.

In addition to theta power, cM1 alpha power was positively associated with motor learning. Motor cortical alpha oscillations show similar modulation as beta oscillations during voluntary movement, ie. ERD during movement anticipation and execution and ERS in the absence of motor output (Pfurtscheller et al., 1996). Previous research with simultaneous EEG/fMRI during a motor task localised alpha-band activity to the post-central cortex, ie. related to processing sensory information. In line with previous research (Pollok et al., 2014; Zhuang et al., 1997), the positive relationship in the alpha band power and learning could reflect lower demand for sensory processing with skill acquisition.

In contrast with previous reports, we did not observe a relationship between M1 beta power and learning; the time-frequency decompositions during both motor tasks showed ERS during rest, ERD during motor execution, and a burst of ERS after the movement ended. It has been suggested that beta ERS represents a state of maintenance of the current motor plan, while beta ERD may be an adaptive state that enables learning Engel and Fries (2010). Furthermore, beta activity is also suggested to be involved in working memory and information processing Spitzer and Haegens (2017). Following Engel and Fries (2010), enhanced beta suppression would be expected to coincide with better learning. This idea is supported by clinical studies with Parkinson's disease (PD) patients, who exhibit less M1 beta suppression and have reduced motor learning capacity (Meissner et al., 2018; Meziane et al., 2015). Similarly, stroke patients were found to have intact but lower learning capacity compared to healthy controls, accompanied by generally higher beta power (Espenhahn et al., 2020). However, both PD and stroke patients often suffer from motor impairment in general, irrespective of learning capacity. Therefore, comparing patients with healthy controls cannot rule out that the identified beta power differences reflect limited motor control instead of limited motor learning.

Within healthy subjects, stronger beta power suppression was also associated with reduced reaction time (Pollok et al., 2014) and faster force production (Joundi et al., 2012). As cM1 beta power suppression results from motor output (Pfurtscheller et al., 1996), the relationship between beta suppression and reaction time (Pollok et al., 2014) and force production (Joundi et al., 2012; Pogosyan et al., 2009) could merely relate to changes in motor output. In the motor task we employed, learning requires optimising a motor plan but not increasing

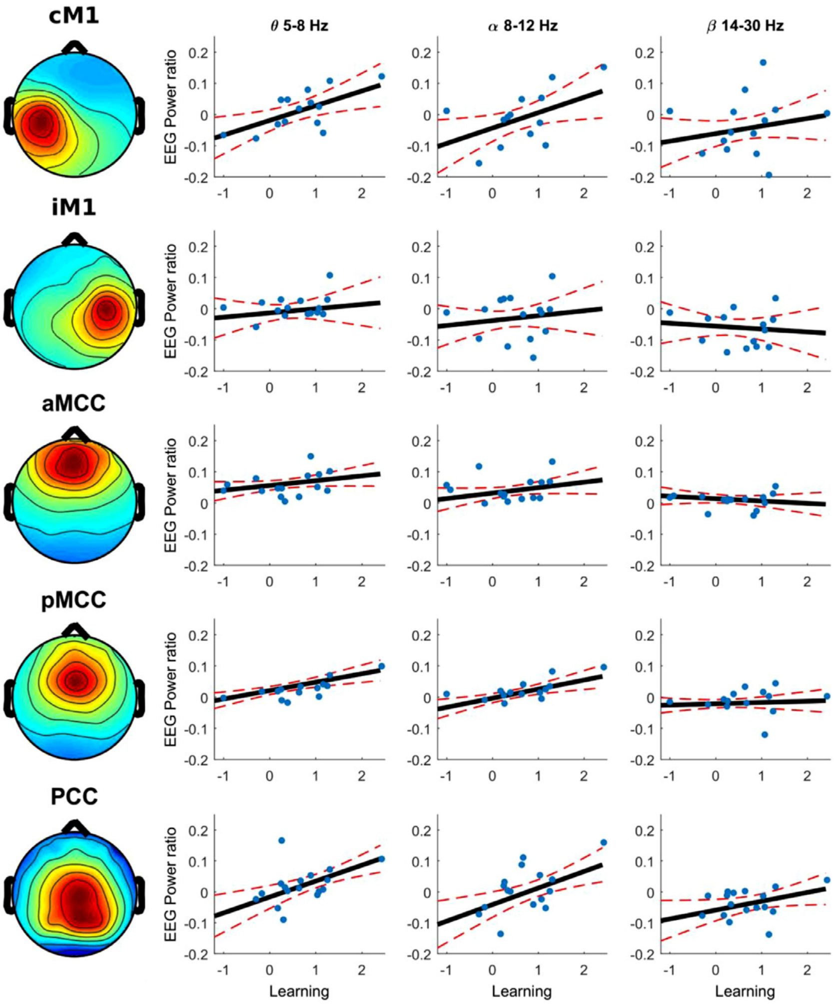

Fig. 4. Cluster-wise visualisation of the marginal effects between the degree of motor learning and the EEG band power ratio during task execution (t = [0, 3.75] minus 1. Column 1 shows scalp maps of corresponding clusters; columns 2–4 show theta, alpha, and beta band power ratios minus 1 (y axis) vs differences in learning slopes between CMT and SMT (x axis). Black lines show the marginal effects of the presented data; blue circles represent the individual data points, and the red lines the 95% confidence intervals of the estimated relationship.

force output or reaction time. By constraining the timing of both motor learning tasks with the metronome and controlling for motor force output with the SMT, the current study finds no relationship between motor learning and beta power.

An additional explanation for the lack of a relation between cM1 beta power and learning may be the time point at which we considered beta power since we considered beta power only during trial execution and not during the post-movement beta rebound. After voluntary movement, beta power typically shows a burst of ERS. This post-movement beta power has been associated with adjustments in motor plans (Schmidt et al., 2019; Tan et al., 2016) and (Espenhahn et al., 2020) but was currently not analysed.

There was less bilateral M1 beta ERD during execution of the SMT compared to the CMT, but individual differences in beta ERD did not correlate with differences in learning. Reduced iM1 beta ERD has previously been linked to lower perceived task difficulty in younger subjects than elderly (Rossiter et al., 2014) and motor performance in healthy subjects compared to elderly (Espenhahn et al., 2019). During unimanual motor tasks in right-handed subjects, the ipsilateral (right) hemisphere functions as a feedback processing system, whereas the contralateral (left) hemisphere acts as a feedforward predictive system (Davare et al., 2007; Mutha et al., 2013). Thus, the amount of iM1 beta ERD may be related to perceived difficulty through increased reliance on supportive mechanisms during the CMT compared to the SMT. In line with this possibility, a combination of interindividual differences in motor learning capacity and perceived difficulty may explain why motor learning was unrelated to iM1 beta power in our study. Nonetheless, we would expect a reduction in ipsilateral beta ERD within subjects over a longer learning period in the CMT, although this was not investigated.

4.2. CC regions

Three additional clusters were localised to subregions of the CC, which is frequently associated with feedback processing (Shenhav et al., 2013). The role of the MCC or dorsal ACC is typically analysed by measuring scalp activity of the Fz or FCz electrode (Cohen et al., 2011). Through ICA combined with dipole fitting, we unexpectedly detected motor learning-related source-level activity in 2 additional, different CC subregions with different time-frequency patterns. These CC subregions have been previously investigated, but primarily using neuroimaging methods such as positron emission tomography (PET) and fMRI (Ball et al., 1999; Jueptner et al., 1997; Picard and Strick, 1996) and less on an electrophysiologic level by EEG (Herrojo Ruiz et al., 2017)or MEG.

The most apparent between-task differences in time-frequency decompositions were found in the aMCC—namely, theta and alpha ERS throughout the execution phase during the CMT but absent during the SMT. During the CMT this ERD was observed in the high-frequency beta range (21–30 Hz), whereas during the SMT, low-frequency beta ERD (14–20 Hz) was more apparent. The aMCC's activity was approximated to originate from the anterior cingulate motor area (Picard and Strick, 1996), which is activated before M1 in motor control (Ball et al., 1999); moreover, the activity is thought to be related to attentional processes (Jueptner et al., 1997). No relationship was found between any of the frequency bands in this cluster and motor learning. Therefore, the between-task EEG differences in the aMCC are likely related solely to the different demands that the CMT and SMT place on attention, working memory, and motor control to achieve good performance.

The pMCC is often associated with performance monitoring and feedback processing, which appeared in time-frequency decompositions through theta ERS bursts (Cohen et al., 2011) that time-locked to the 750 ms interval of the metronome that indicated when the cursor had to reach the target location. As such, the observed association between theta power and motor learning may reflect the importance of feedback on performance and errors during the learning of a complex motor task. Furthermore, the alpha band—which is often associated with attentional demands and memory Klimesch (1997)— was positively associated with motor learning. As a mechanism underlying feedback processing, higher pMCC theta power has been linked to increased connectivity to other brain regions such as M1 Cohen (2011). As such, higher theta power may drive motor learning through more efficient processing of visual feedback on performance and interact with M1 to enable adjustment of motor control. The positive association between alpha power and learning was unexpected, as it did not support the theory that alpha power suppression is proportional to increases in attentional demand, which would be expected in the CMT as compared to the SMT (Klimesch, 1999). However, it has also been suggested that attention and memory are modulated by different sub-bands of the alpha band Klimesch (1997). Thus, it is possible that greater alpha power suppression during the SMT reflects an increased reliance on memory retrieval to maintain high performance. In contrast, less suppression during learning in the CMT corresponds to motor plan adjustments.

Finally, the third identified cluster in the CC was localised to the PCC, which is part of the default mode network and plays an important role in cognition, attention and memory Leech and Sharp (2014). In the PCC, alpha ERD bursts preceded the metronome ticks theta ERS bursts succeeded the metronome, suggesting distinct functions for the theta and alpha band related to retrieving/encoding task-related memory (Kim et al., 2020) or attentional processes (Cona et al., 2020). Cona et al. (2020) suggest that increased theta ERS reflects internally directed attention and alpha ERD external attention. Consequently, participants who learn better might require less external information during the task, such as auditory cues or visual feedback. However, additional analyses are needed to understand how theta and alpha power are related to each other and learning.

4.3. Limitations

Our results were acquired by analysing EEG data recorded during a complex and simple explicit motor learning task. Therefore, it is unclear whether our results generalise to other motor learning task types such as adaptation learning or implicit learning. Furthermore, EEG records only cortical activity, although motor learning also involves subcortical structures such as the basal ganglia (Doyon et al., 2009). We acquired our results by applying ICA-based source reconstruction, through which we identified task-related cortical activity localised to M1 and 3 clusters in the CC. A limitation of ICA is that none of the constructed clusters included all participants in the study, which reduced the statistical power of an already small sample size. Furthermore, the identified brain regions were determined by dipole fitting of independent components in a three-shell head model based on the MNI template brain model with default conductivity values for scalp, skull, CSF and brain. However, intersubject variability in anatomy and particularly skull conductivity (McCann et al., 2019) influence dipole fitting accuracy (Vorwerk et al., 2019). For the M1 clusters, the source reconstruction provided time-frequency decompositions typically observed during motor tasks, verifying the dipole localisation. However, this was not possible for the CC clusters due to the limited availability of electrophysiologic time-frequency activations in these regions. Only error-related theta modulation around the metronome ticks was available as a reference to verify the pMCC cluster's location. Given these limitations, our study results should be taken as exploratory. Nonetheless, they provide a basis for more hypothesis-driven research to elucidate the EEG correlates of motor learning.

5. Conclusion

This study shows that – controlling for performing a movement – contralateral M1 theta and alpha but not beta power are positively associated with motor learning, as are theta and alpha power in the pMCC and PCC. In the beta band, M1 suppression was stronger during the CMT than during the SMT, but this was not associated with a higher degree of motor learning. Our findings support theta and alpha oscillations' involvement in learning a complex, explicit motor task, possibly by enhancing communication between distant cortical regions, error monitoring and attentional processes. Furthermore, they suggest that M1 beta power merely relates to interindividual differences in the capability of performing but not learning a motor task. We propose that further analysis of theta cross-frequency interactions between M1, CC regions and the basal ganglia may provide additional insight into the electrophysiologic basis of complex motor learning .

Data and code availability statement

The data that support the findings of this study are available from the corresponding author, JC, upon reasonable request.

Declaration of Competing Interest

None.

Credit authorship contribution statement

Joris van der Cruijsen: Conceptualization, Methodology, Formal analysis, Investigation, Data curation, Writing – original draft, Visualization. **Mana Manoochehri:** Conceptualization, Methodology, Formal analysis, Investigation, Writing – original draft. **Zeb D. Jonker:** Conceptualization, Methodology, Software, Visualization, Writing – review & editing. **Eleni-Rosalina Andrinopoulou:** Formal analysis, Writing – review & editing. **Maarten A. Frens:** Writing – review & editing, Funding acquisition. **Gerard M. Ribbers:** Writing – review & editing, Funding acquisition. **Alfred C. Schouten:** Writing – review & editing, Funding acquisition. **Ruud W. Selles:** Resources, Writing – review & editing, Supervision, Funding acquisition.

Acknowledgments

We would like to thank Yvonne Greeuw for her contribution to the experimental design and data collection and Jessica Wijngaarden for her help during the data collection. This manuscript was edited for English Language by Charlesworth Author Services (www.cwauthors.com).

Funding

This study was supported by the Netherlands Organisation of Scientific Research (NWO), domain Applied and Engineering Science (TTW): NeuroCIMT-itDCS: project number 14902.

Supplementary materials

Supplementary material associated with this article can be found, in the online version, at doi:10.1016/j.neuroimage.2021.118373.

References

Akkad, H., Dupont-Hadwen, J., Frese, A., Tetkovic, I., Barrett, L., Bestmann, S., Stagg, C., 2019. Increasing motor skill acquisition by driving theta-gamma coupling. bioRxiv. https://doi.org/ 10.1101/2019.12.20.883926

Amo, C., De Santiago, L., Luciáñez, D.Z., Alonso-Cortés, J.M.L., Alonso-Alonso, M., Barea, R., Boquete, L., 2017. Induced gamma band activity from EEG as a possible index of training-related brain plasticity in motor tasks. PLoS ONE 12. doi:10.1371/journal.pone.0186008, e0186008–e0186008https://doi.org/.

Arthur, D., Vassilvitskii, S., 2007. K-means++: the advantages of careful seeding. In: Proceedings of the Annual ACM-SIAM Symposium on Discrete Algorithms, pp. 1027–1035.

Ashe, J., Lungu, O.V., Basford, A.T., Lu, X., 2006. Cortical control of motor sequences. Curr. Opin. Neurobiol. 16, 213–221. doi:10.1016/j.conb.2006.03.008, https://doi.org/.

Ball, T., Schreiber, A., Feige, B., Wagner, M., Lücking, C.H., Kristeva-Feige, R., 1999. The role of higher-order motor areas in voluntary movement as revealed by high-resolution EEG and fMRI. Neuroimage 10, 682–694. doi:10.1006/nimg.1999.0507, https://doi.org/.

Boonstra, T.W., Daffertshofer, A., Breakspear, M., Beek, P.J., 2007. Multivariate time-frequency analysis of electromagnetic brain activity during bimanual motor learning. Neuroimage 36, 370–377. doi:10.1016/j.neuroimage.2007.03.012, https://doi.org/.

Brittain, J.S., Brown, P., 2014. Oscillations and the basal ganglia: motor control and beyond. Neuroimage doi:10.1016/j.neuroimage.2013.05.084, https://doi.org/.

Canolty, R.T., Edwards, E., Dalal, S.S., Soltani, M., Nagarajan, S.S., Kirsch, H.E., Berger, M.S., Barbare, N.M., Knight, R.T., 2006. High gamma power is phase-locked to theta oscillations in human neocortex. Science 313, 1626–1628. doi:10.1126/science.1128115, https://doi.org/.

Caplan, J.B., Madsen, J.R., Schulze-Bonhage, A., Aschenbrenner-Scheibe, R., Newman, E.L., Kahana, M.J., 2003. Human θ oscillations related to sensorimotor integration and spatial learning. J. Neurosci. 23, 4726–4736. doi:10.1523/jneurosci.23-11-04726.2003, https://doi.org/.

Chacko, R.V., Kim, B., Jung, S.W., Daitch, A.L., Roland, J.L., Metcalf, N.V., Corbetta, M., Shulman, G.L., Leuthardt, E.C., 2018. Distinct phase-amplitude couplings distinguish cognitive processes in human attention. Neuroimage 175, 111–121. doi:10.1016/j.neuroimage.2018.03.003, https://doi.org/.

Cohen, M.X., 2011. Error-related medial frontal theta activity predicts cingulate-related structural connectivity. Neuroimage 55, 1373–1383. doi:10.1016/j.neuroimage.2010.12.072, https://doi.org/.

Cohen, M.X., Wilmes, K., van de Vijver, I., 2011. Cortical electrophysiological network dynamics of feedback learning. Trends Cogn. Sci. (Regul. Ed.) 15, 558–566. doi:10.1016/j.tics.2011.10.004, https://doi.org/.

Cona, G., Chiossi, F., Di Tomasso, S., Pellegrino, G., Piccione, F., Bisiacchi, P., Arcara, G., 2020. Theta and alpha oscillations as signatures of internal and external attention to delayed intentions: a magnetoencephalography (MEG) study. Neuroimage 205, 116295. doi:10.1016/j.neuroimage.2019.116295, https://doi.org/.

Coxon, J.P., Peat, N.M., Byblow, W.D., 2014. Primary motor cortex disinhibition during motor skill learning. J. Neurophysiol. 112, 156–164. doi:10.1152/jn.00893.2013, https://doi.org/.

Davare, M., Duque, J., Vandermeeren, Y., Thonnard, J.L., Olivier, E., 2007. Role of the ipsilateral primary motor cortex in controlling the timing of hand muscle recruitment. Cerebral Cortex 17, 353–362. doi:10.1093/cercor/bhj152, https://doi.org/.

Delorme, A., Makeig, S., 2004. EEGLAB: an open source toolbox for analysis of single-trial EEG dynamics including independent component analysis. J. Neurosci. Methods 134, 9–21. doi:10.1016/j.jneumeth.2003.10.009, https://doi.org/.

Delorme, A., Palmer, J., Onton, J., Oostenveld, R., Makeig, S., 2012. Independent EEG sources are dipolar. PLoS ONE 7. doi:10.1371/journal.pone.0030135, e30135–e30135https://doi.org/.

Doyon, J., Bellec, P., Amsel, R., Penhune, V., Monchi, O., Carrier, J., Lehéricy, S., Benali, H., 2009. Contributions of the basal ganglia and functionally related brain structures to motor learning. Behav. Brain Res. doi:10.1016/j.bbr.2008.11.012, https://doi.org/.

Engel, A.K., Fries, P., 2010. Beta-band oscillations–signalling the status quo? Curr. Opin. Neurobiol. 20 156–165–156–165.

Espenhahn, S., Rossiter, H.E., van Wijk, B.C.M., Redman, N., Rondina, J.M., Diedrichsen, J., Ward, N.S., 2020. Sensorimotor cortex beta oscillations reflect motor skill learning ability after stroke. Brain Commun. 2. doi:10.1093/braincomms/fcaa161, https://doi.org/.

Espenhahn, S., van Wijk, B.C.M., Rossiter, H.E., de Berker, A.O., Redman, N.D., Rondina, J., Diedrichsen, J., Ward, N.S., 2019. Cortical beta oscillations are associated with motor performance following visuomotor learning. Neuroimage 195, 340–353. doi:10.1016/j.neuroimage.2019.03.079, https://doi.org/.

Ghilardi, M.F., Ghez, C., Dhawan, V., Moeller, J., Mentis, M., Nakamura, T., Antonini, A., Eidelberg, D., 2000. Patterns of regional brain activation associated with different forms of motor learning. Brain Res. 871, 127–145. doi:10.1016/S0006-8993(00)02365-9, https://doi.org/.

Grandchamp, R., Delorme, A., 2011. Single-trial normalization for event-related spectral decomposition reduces sensitivity to noisy trials. Front. Psychol. 2, 236. doi:10.3389/fpsyg.2011.00236, https://doi.org/.

Guerra, A., Asci, F., D'Onofrio, V., Sveva, V., Bologna, M., Fabbrini, G., Berardelli, A., Suppa, A., 2020. Enhancing gamma oscillations restores primary motor cortex plasticity in Parkinson's disease. J. Neurosci. 40, 4788–4796. doi:10.1523/JNEUROSCI.0357-20.2020, https://doi.org/.

Halekoh, U., Højsgaard, S., Yan, J., 2006. The R package geepack for generalized estimating equations. J. Stat. Softw. doi:10.18637/jss.v015.i02, https://doi.org/.

Herrojo Ruiz, M., Maess, B., Altenmüller, E., Curio, G., Nikulin, V.V., 2017. Cingulate and cerebellar beta oscillations are engaged in the acquisition of auditory-motor sequences. Hum Brain Mapp 38, 5161–5179. doi:10.1002/hbm.23722, https://doi.org/.

Hubbard, A.E., Ahern, J., Fleischer, N.L., Laan, M.Van Der, Lippman, S.A., Jewell, N., Bruckner, T., Satariano, W.A., 2010. To GEE or not to GEE: comparing population average and mixed models for estimating the associations between neighborhood risk factors and health. Epidemiology doi:10.1097/EDE.0b013e3181caeb90, https://doi.org/.

Joundi, R.A., Jenkinson, N., Brittain, J.S., Aziz, T.Z., Brown, P., 2012. Driving oscillatory activity in the human cortex enhances motor performance. Curr. Biol. 22, 403–407. doi:10.1016/j.cub.2012.01.024, https://doi.org/.

Jueptner, M., Stephan, K.M., Frith, C.D., Brooks, D.J., Frackowiak, R.S.J., Passingham, R.E., 1997. Anatomy of motor learning. I. Frontal cortex and attention to action. J. Neurophysiol. 77, 1313–1324. doi:10.1152/jn.1997.77.3.1313, https://doi.org/.

Kim, D., Jeong, W., Kim, J.S., Chung, C.K., 2020. Single-trial EEG connectivity of default mode network before and during encoding predicts subsequent memory outcome. Front Syst Neurosci 14, 86. doi:10.3389/fnsys.2020.591675, https://doi.org/.

Klimesch, W., 1997. EEG-alpha rhythms and memory processes. Int. J. Psychophysiol. 26, 319–340. doi:10.1016/S0167-8760(97)00773-3, https://doi.org/.

Klimesch, W., 1999. EEG alpha and theta oscillations reflect cognitive and memory performance: A review and analysis. Brain Res. Rev. 29, 169–195. doi:10.1016/S0165-0173(98)00056-3.

Lancaster, J.L., Rainey, L.H., Summerlin, J.L., Freitas, C.S., Fox, P.T., Evans, A.C., Toga, A.W., Mazziotta, J.C., 1997. Automated labeling of the human brain: a preliminary report on the development and evaluation of a forward-transform method. Hum. Brain Mapp. 5, 238–242 https://doi.org/10.1002/(SICI)1097-0193(1997)5:4<238::AID-HBM6>3.0.CO;2-4.

Lancaster, J.L., Woldorff, M.G., Parsons, L.M., Liotti, M., Freitas, C.S., Rainey, L., Kochunov, P.V., Nickerson, D., Mikiten, S.A., Fox, P.T., 2000. Automated Talairach atlas labels for functional brain mapping. Hum Brain Mapp 10, 120–131 https://doi.org/10.1002/1097-0193(200007)10:3<120::AID−HBM30>3.0.CO;2-8.

Leech, R., Sharp, D.J., 2014. The role of the posterior cingulate cortex in cognition and disease. Brain 137, 12–32. doi:10.1093/brain/awt162, https://doi.org/.

Magill, R., Anderson, D., 2017. Motor Learning and control : Concepts and Applications /Richard A. Magill. McGraw-Hill Education, New York, NY.

Mane, R., Chew, E., Phua, K.S., Ang, K.K., Robinson, N., Vinod, A.P., Guan, C., 2019. Prognostic and monitory EEG-biomarkers for BCI upper-limb stroke rehabilitation. IEEE Trans. Neural Syst. Rehabil. Eng. 27, 1654–1664. doi:10.1109/TNSRE.2019.2924742, https://doi.org/.

McCann, H., Pisano, G., Beltrachini, L., 2019. Variation in reported human head tissue electrical conductivity values. Brain Topogr 32, 825–858. doi:10.1007/s10548-019-00710-2, https://doi.org/.

McHughen, S.A., Rodriguez, P.F., Kleim, J.A., Kleim, E.D., Crespo, L.M., Procaccio, V., Cramer, S.C., 2010. BDNF val66met polymorphism influences motor system function in the human brain. Cerebral Cortex 20, 1254–1262. doi:10.1093/cercor/bhp189, https://doi.org/.

Meissner, S.N., Krause, V., Südmeyer, M., Hartmann, C.J., Pollok, B., 2018. The significance of brain oscillations in motor sequence learning: insights from Parkinson's disease. NeuroImage 20, 448–457. doi:10.1016/j.nicl.2018.08.009, https://doi.org/.

Meziane, H.B., Moisello, C., Perfetti, B., Kvint, S., Isaias, I.U., Quartarone, A., Rocco, A.Di, Ghilardi, M.F., 2015. Movement preparation and bilateral modulation of beta activity in aging and Parkinson's disease. PLoS ONE 10. doi:10.1371/journal.pone.0114817, e0114817–e0114817https://doi.org/.

Mutha, P.K., Haaland, K.Y., Sainburg, R.L., 2013. Rethinking motor lateralization: specialized but complementary mechanisms for motor control of each arm. PLoS ONE 8. doi:10.1371/journal.pone.0058582, e58582–e58582https://doi.org/.

Nowak, M., Zich, C., Stagg, C.J., 2018. Motor cortical gamma oscillations: what have we learnt and where are we headed? Curr Behav Neurosci Rep 5, 136–142. doi:10.1007/s40473-018-0151-z, https://doi.org/.

Oostenveld, R., Praamstra, P., 2001. The five percent electrode system for high-resolution EEG and ERP measurements. Clin. Neurophysiol. 112, 713–719. doi:10.1016/S1388-2457(00)00527-7, https://doi.org/.

Osipova, D., Hermes, D., Jensen, O., 2008. Gamma power is phase-locked to posterior alpha activity. PLoS ONE 3, e3990. doi:10.1371/journal.pone.0003990, https://doi.org/.

Palmer, J.A., Makeig, S., Kreutz-Delgado, K., Rao, B.D., 2008. Newton method for the ICA mixture model. In: ICASSP, IEEE International Conference on Acoustics, Speech and Signal Processing - Proceedings. IEEE, pp. 1805–1808. doi:10.1109/ICASSP.2008.4517982 https://doi.org/.

Pellegrino, G., Tomasevic, L., Herz, D.M., Larsen, K.M., Siebner, H.R., 2018. Theta activity in the left dorsal premotor cortex during action re-evaluation and motor reprogramming. Front. Hum. Neurosci. 12, 364. doi:10.3389/fnhum.2018.00364, https://doi.org/.

Pfurtscheller, G., Stancák, A., Neuper, C., 1996. Post-movement beta synchronization. A correlate of an idling motor area? Electroencephalogr Clin. Neurophysiol. 98, 281–293. doi:10.1016/0013-4694(95)00258-8, https://doi.org/.

Picard, N., Strick, P.L., 1996. Motor areas of the medial wall: a review of their location and functional activation. Cerebral Cortex 6, 342–353. doi:10.1093/cercor/6.3.342, https://doi.org/.

Pinheiro, J., Bates, D., DebRoy, S., Sarkar, D., R Core Team, 2020. nlme: linear and Nonlinear Mixed Effects Models [WWW Document]. URL https://cran.r-project.org/package=nlme

Pogosyan, A., Gaynor, L.D., Eusebio, A., Brown, P., 2009. Boosting cortical activity at beta-band frequencies slows movement in humans. Curr. Biol. 19, 1637–1641. doi:10.1016/j.cub.2009.07.074, https://doi.org/.

Pollok, B., Latz, D., Krause, V., Butz, M., Schnitzler, A., 2014. Changes of motor-cortical oscillations associated with motor learning. Neuroscience 275, 47–53. doi:10.1016/j.neuroscience.2014.06.008, https://doi.org/.

Reis, J., Schambra, H.M., Cohen, L.G., Buch, E.R., Fritsch, B., Zarahn, E., Celnik, P.A., Krakauer, J.W., 2009. Noninvasive cortical stimulation enhances motor skill acquisition over multiple days through an effect on consolidation. Proc. Natl. Acad. Sci. USA 106, 1590–1595. doi:10.1073/pnas.0805413106, https://doi.org/.

Rossiter, H.E., Davis, E.M., Clark, E.V., Boudrias, M.H., Ward, N.S., 2014. Beta oscillations reflect changes in motor cortex inhibition in healthy ageing. Neuroimage 91, 360–365. doi:10.1016/j.neuroimage.2014.01.012, https://doi.org/.

Rozengurt, R., Barnea, A., Uchida, S., Levy, D.A., 2016. Theta EEG neurofeedback benefits early consolidation of motor sequence learning. Psychophysiology 53, 965–973. doi:10.1111/psyp.12656, https://doi.org/.

Saha, S., Baumert, M., 2020. Intra- and inter-subject variability in EEG-based sensorimotor brain computer interface: a review. Front Comput Neurosci 13, 87. doi:10.3389/fncom.2019.00087, https://doi.org/.

Schmidt, R., Ruiz, M.H., Kilavik, B.E., Lundqvist, M., Starr, P.A., Aron, A.R., 2019. Beta oscillations in working memory, executive control of movement and thought, and sensorimotor function. J. Neurosci. Soc. Neurosci. 8231–8238. doi:10.1523/JNEUROSCI.1163-19.2019, https://doi.org/.

Shenhav, A., Botvinick, M.M., Cohen, J.D., 2013. The expected value of control: an integrative theory of anterior cingulate cortex function. Neuron 79, 217–240. doi:10.1016/j.neuron.2013.07.007, https://doi.org/.

Spitzer, B., Haegens, S., 2017. Beyond the status quo: a role for beta oscillations in endogenous content (RE)activation. eNeuro. https://doi.org/ 10.1523/ENEURO.0170-17.2017

Sugata, H., Yagi, K., Yazawa, S., Nagase, Y., Tsuruta, K., Ikeda, T., Matsushita, K., Hara, M., Kawakami, Kenji, Kawakami, Keisuke, 2018. Modulation of motor learning capacity by transcranial alternating current stimulation. Neuroscience 391, 131–139. doi:10.1016/j.neuroscience.2018.09.013, https://doi.org/.

Tan, H., Wade, C., Brown, P., 2016. Post-movement beta activity in sensorimotor cortex indexes confidence in the estimations from internal models. J. Neurosci. 36, 1516–1528. doi:10.1523/JNEUROSCI.3204-15.2016, https://doi.org/.

Thut, G., Bergmann, T.O., Fröhlich, F., Soekadar, S.R., Brittain, J.S., Valero-Cabré, A., Sack, A.T., Miniussi, C., Antal, A., Siebner, H.R., Ziemann, U., Herrmann, C.S., 2017. Guiding transcranial brain stimulation by EEG/MEG to interact with ongoing brain activity and associated functions: a position paper. Clin. Neurophysiol. 128, 843–857. doi:10.1016/j.clinph.2017.01.003, https://doi.org/.

Tomassini, V., Jbabdi, S., Kincses, Z.T., Bosnell, R., Douaud, G., Pozzilli, C., Matthews, P.M., Johansen-Berg, H., 2011. Structural and functional bases for individual differences in motor learning. Hum Brain Mapp. 32, 494–508. doi:10.1002/hbm.21037, https://doi.org/.

Vogt, B.A., 2016. Midcingulate cortex: structure, connections, homologies, functions and diseases. J. Chem. Neuroanat. 74, 28–46.

Vorwerk, J., Aydin, Ü., Wolters, C.H., Butson, C.R., 2019. Influence of head tissue conductivity uncertainties on EEG dipole reconstruction. Front Neurosci 13, 531. doi:10.3389/fnins.2019.00531, https://doi.org/.

Weiss, D., Klotz, R., Govindan, R.B., Scholten, M., Naros, G., Ramos-Murguialday, A., Bunjes, F., Meisner, C., Plewnia, C., Kruger, R., Gharabaghi, A., 2015. Subthalamic stimulation modulates cortical motor network activity and synchronization in Parkinson's disease. Brain 138, 679–693. doi:10.1093/brain/awu380, https://doi.org/.

Zhuang, P., Toro, C., Grafman, J., Manganotti, P., Leocani, L., Hallett, M., 1997. Event-related desynchronization (ERD) in the alpha frequency during development of implicit and explicit learning. Electroencephalogr Clin Neurophysiol 102, 374–381. doi:10.1016/S0013-4694(96)96030-7, https://doi.org/.